IOSR Journal of Mechanical and Civil Engineering (IOSR-JMCE)
e-ISSN: 2278-1684, p-ISSN: 2320-334X, Volume 23, Issue 6 Ser. I (Nov. – Dec. 2026), PP 10-19
www.iosrjournals.org

Condition-Based Assessment and Micro-Concrete Jacketing of Corrosion-Damaged RC Columns in Low-Rise Buildings: An ETABS-Supported Case Study from Mumbai

Shahnawaz Ukaye[1], Dr. Dada S. Patil[2], Dr. Shaikh Irfan[3], Afroz Khan[4]
[1]Department of Civil Engineering, School of Engineering and Technology, Anjuman-I-Islam's Kalsekar Technical Campus, New Panvel, Navi Mumbai 410206, Maharashtra, India (Affiliated to the University of Mumbai)

Abstract: *Many low-rise reinforced concrete (RC) buildings in coastal Mumbai reach the middle of their service life with corroded column bars, spalled cover and concrete grades that are now below the code minimum. This paper examines a three-storey RC cold-storage building in Andheri built with M15 concrete and 225 mm × 525 mm columns. A staged protocol is followed, combining visual survey, rebound hammer and ultrasonic pulse velocity (UPV) testing, a linear static and modal audit in ETABS under IS 1893 (Part 1):2016 and IS 875 (Part 3), and a strain-compatibility check of the critical column at four corrosion states. A second four-storey frame audited the same way is included for comparison. The audit showed that inter-storey drifts of the case building stay below 0.65 × 10⁻³, far inside the 0.004 limit, but the building is torsionally irregular in the X direction (Δmax/Δavg up to 1.33) and its first mode carries 24 percent torsional mass. The comparison frame revealed a soft ground storey with only 31 percent of the upper-storey stiffness and a drift of 0.0089. At the member level, the intact column carries the 1037 kN factored demand (axial demand-capacity ratio 0.90), but 25 percent bar section loss with cover spalling lifts the ratio to 1.12 and fails the biaxial check. A 75 mm M35 micro-concrete jacket raises the design axial capacity to 3086 kN after a 0.9 monolithic factor. Deterioration, not original design, governs the retrofit need.*

Keywords: *RC column jacketing; micro-concrete; reinforcement corrosion; ETABS structural audit; torsional irregularity; soft storey; IS 15988*

Date of Submission: 27-10-2026 Date of Acceptance: 06-11-2026

I. Introduction

A large part of the urban RC stock in India was built between the 1980s and the early 2000s, when M15 concrete, nominal cover and non-ductile detailing were routine. In coastal cities such as Mumbai the combined effect of chloride-laden air, high humidity and carbonation shortens the corrosion initiation period, and owners typically call an engineer only after cover has cracked or spalled. At that stage the engineer has to decide two things quickly: whether the frame as a whole is adequate under current codes, and how much of the lost member capacity must be restored.

Column jacketing remains the most widely used answer to the second question. Recent reviews place reinforced concrete jacketing, steel caging, fibre-reinforced polymer (FRP) wraps and fibre-reinforced cementitious matrices side by side and conclude that concrete jacketing is still the most economical choice where a modest increase in section size is acceptable [1]-[3]. Experimental work since 2022 has focused heavily on corrosion. Aminulai et al. tested ageing low-strength columns and found that axial capacity and ductility drop sharply once tie corrosion removes confinement and longitudinal bars start to buckle [4], [5]. Chen et al. linked crack growth to residual capacity in eccentrically loaded corroded columns within a reliability framework [6], while Dai et al. showed that FRP retrofit restores strength but leaves deformation capacity sensitive to the original corrosion level [7]. Thin high-performance jackets have drawn particular attention. UHPC and UHPFRC jackets on corroded or pre-damaged columns recovered or exceeded the original capacity and slowed further corrosion [8]-[11], and recent tests on thin HPFRC jackets and hybrid mortar and CFRP jackets point the same way [12]-[14]. Earlier seismic tests with UHPFRC jackets [15] support these findings under cyclic loading.

For field repairs in India, however, the jacket material is almost always a pre-bagged, shrinkage-compensated flowable micro-concrete rather than UHPFRC. Its performance depends heavily on early-age shrinkage and bond with the old substrate. Nayak et al. measured relative shrinkage of six commercial micro-concretes and showed that bond strength, more than free shrinkage alone, governs interface cracking [16]. Baloch et al. [17] and two recent reviews on old-to-new concrete bond [18], [19] reach similar conclusions on surface roughness, moisture state and restraint.

At the building level, numerical audits of existing Indian frames have mostly examined code revisions and retrofit alternatives in seismic zones IV and V [20], [21]. Few published cases connect a routine ETABS audit, the corrosion state of individual columns and the design of a practical micro-concrete jacket within one decision path. This gap is addressed here. The specific objectives are to (i) audit a three-storey M15 building for drift, torsion and modal behaviour under current Indian codes, (ii) contrast the outcome with a second frame that has a stiffness irregularity, (iii) quantify how bar section loss and cover spalling move the critical column across the adequacy boundary, and (iv) size and check a micro-concrete jacket against IS 456:2000 and IS 15988:2013.

II. Case-Study Buildings and Assessment Protocol

2.1 Description of the buildings

Frame A is a three-storey RC cold-storage building in Andheri, Mumbai. The plan measures 13.37 m × 25.635 m on four grid lines in X (bays of 6.37 m, 3.75 m and 3.25 m) and ten in Y (bays of 2.15 m to 3.125 m), with a uniform storey height of 3.0 m. All 30 columns and all beams are 225 mm × 525 mm, the slab is 200 mm thick, and the as-built concrete and steel are M15 and HYSD Fe415. The structural model is shown in Fig. 1. Frame B is a four-storey RC frame of 30 m × 9 m in plan with 3.0 m storeys. It was audited with the same workflow and is used only to illustrate how the audit responds to a different kind of deficiency.

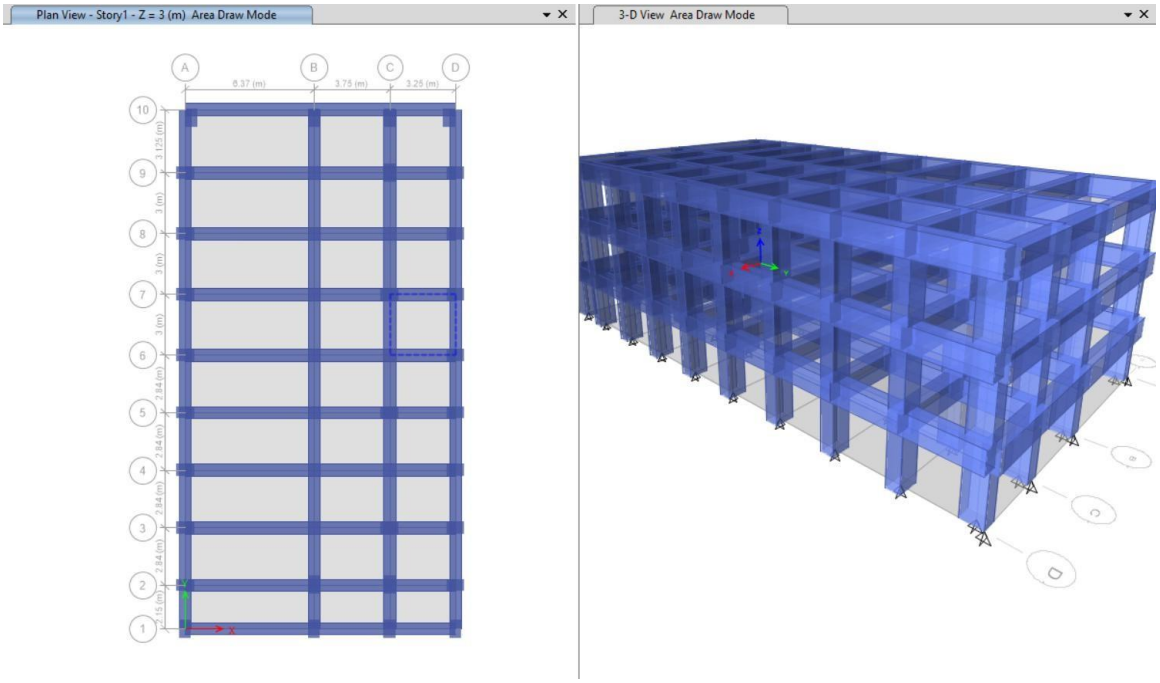


Fig. 1. ETABS model of Frame A: Storey 1 plan with column layout (left) and three-dimensional view (right).

2.2 Assessment protocol

The work followed the eight stages summarised in Fig. 2. Stages 1 and 2 establish the condition of concrete and steel. Rebound hammer and UPV readings are interpreted together, following the combined approach that has proved more reliable than either test alone, and graded against IS 516 (Part 5/Sec 1):2018 [29]. Stage 3 is the global audit in ETABS. Stage 4 moves to the critical column, where capacity is evaluated for a range of corrosion states rather than a single assumed value. Only if the demand-capacity ratio (DCR) exceeds unity does the protocol proceed to jacket design and execution (Stages 5 and 6). Stages 7 and 8 close the loop with post-repair testing and a maintenance plan.

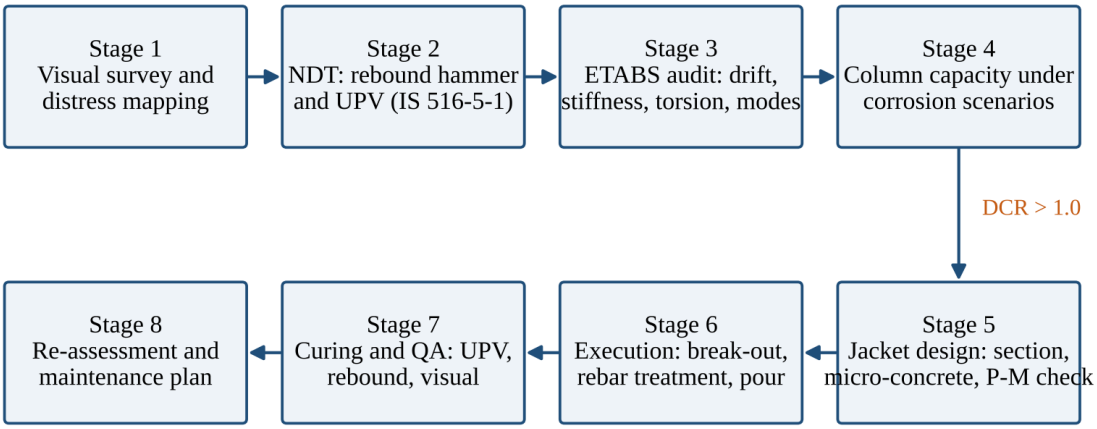


Fig. 2. Staged assessment and repair protocol adopted in this study.



Fig. 3. Site condition of Frame A during surface preparation: spalled cover, exposed and corroded bars along beam soffits and column faces, and scaffolding for the repair.

Visual survey of Frame A recorded spalling of cover along beam soffits and column faces, exposed longitudinal bars with flaking rust, honeycombed patches near construction joints and cracking parallel to the main bars (Fig. 3). The cold-storage use, with its persistent humidity and condensation, is a plausible aggravating factor. The extent of cover loss and bar exposure guided the choice of corrosion scenarios in Section 4.

III. Global Structural Audit

3.1 Modelling and loading

Frame A was modelled in ETABS v22.5 with frame elements for beams and columns, membrane slabs assigned to a rigid diaphragm at each floor and fixed supports at the base. Dead load comprised self-weight, a line load of 2.475 kN/m on beams and 2.875 kN/m on columns representing finishes and services. Wind loads were generated for a basic wind speed of 44 m/s with $k_1 = 1.0$, giving a design wind speed of 43.12 m/s and a design pressure of about 1.12 kN/m². Seismic loads followed the equivalent static method of IS 1893 (Part 1):2016 [26] with Z = 0.36, soil type II and Sa/g = 2.5. The seismic weight was 16,551 kN and the code base shear 1489.6 kN. The lateral load patterns in the model also contained a uniform supplementary area load, so that the applied EQ

X and EQ Y base shear reached 3546 kN. Since Andheri lies in Zone III (Z = 0.16), both choices make the seismic checks conservative by a wide margin. Twenty-six strength combinations of dead, wind and earthquake load were evaluated. Frame B was analysed in ETABS v23.3 with the same load types and combinations.

Under the 1.5DL combination the total vertical reaction of Frame A is 31,850 kN, or 1062 kN per column on average. This figure is consistent with the factored axial demand of 1037 kN adopted later for the critical interior column. Seismic action governs the lateral design: the EQ X base shear is 12.7 times the W X base shear of 278.8 kN.

3.2 Drift and torsional regularity

Fig. 4 presents storey shear, inter-storey drift ratio and the ratio of maximum to average storey displacement for Frame A. The largest drift ratio, 0.648 × 10^{-3} at Storey 2 under EQ X, is about one sixth of the 0.004 limit of IS 1893. Stiffness, in other words, is not a concern for this building. Torsion is. Under EQ X the displacement ratio Δmax/Δavg rises from 1.27 at Storey 1 to 1.33 at the roof, inside the 1.2 to 1.4 band that IS 1893 (Part 1):2016 classifies as torsional irregularity and for which three-dimensional dynamic analysis is mandatory. Under EQ Y the ratio stays near 1.05. The cause lies in the column layout (Fig. 1). Grid B carries columns only near its two ends, several positions on grid C have no column, and the columns at the two short ends are rotated through 90 degrees. As a result, the X-direction stiffness is unevenly spread along the length, and the centre of rigidity sits away from the centre of mass.

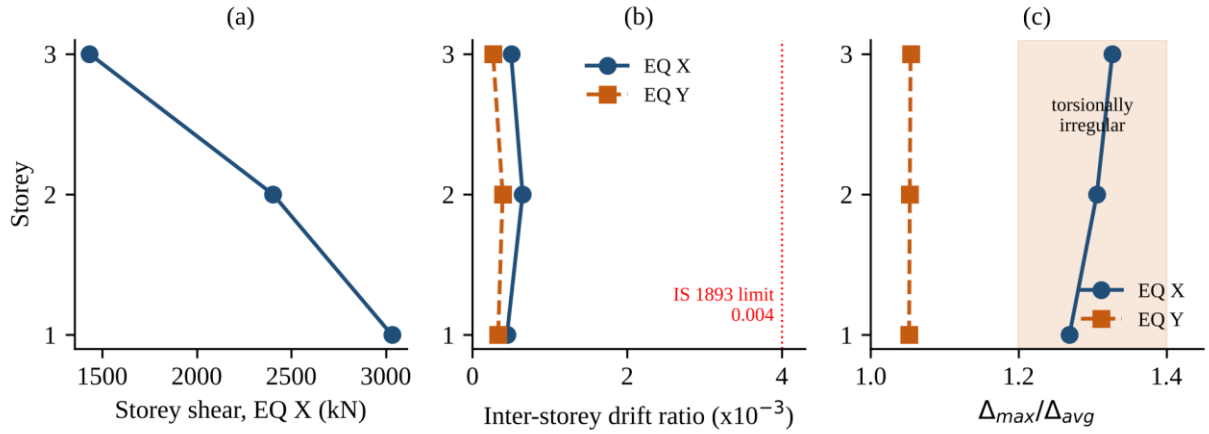


Fig. 4. Frame A under equivalent static seismic load: (a) EQ X storey shear, (b) inter-storey drift ratios against the IS 1893 limit, (c) torsional irregularity ratio.

3.3 Modal behaviour

The modal results confirm the torsional sensitivity (Fig. 5a). The fundamental period of Frame A is 0.246 s, and mode 1 combines 58 percent translational mass in X with 24 percent rotational mass. Mode 2 (0.206 s) is almost purely Y translation and mode 3 (0.182 s) is predominantly torsional. These periods sit close to the empirical value 0.09h/√d of IS 1893 for infilled frames, which gives 0.22 s in X and 0.16 s in Y. Twelve modes captured 99.5 percent and 99.8 percent of the mass in X and Y. The analysis log did flag near-zero modal mass in three high-frequency modes (periods of 0.001 s to 0.002 s), which point to locally ill-conditioned joints in the model. They do not affect the governing modes but should be cleaned up before nonlinear analysis.

Frame B behaves differently. Its first three modes are cleanly uncoupled, with 97.8 percent Y translation in mode 1 (0.776 s), 97.3 percent torsion in mode 2 and 96.0 percent X translation in mode 3 (Fig. 5b). Its displacement ratios remain below 1.03. Torsion is not the issue for Frame B.

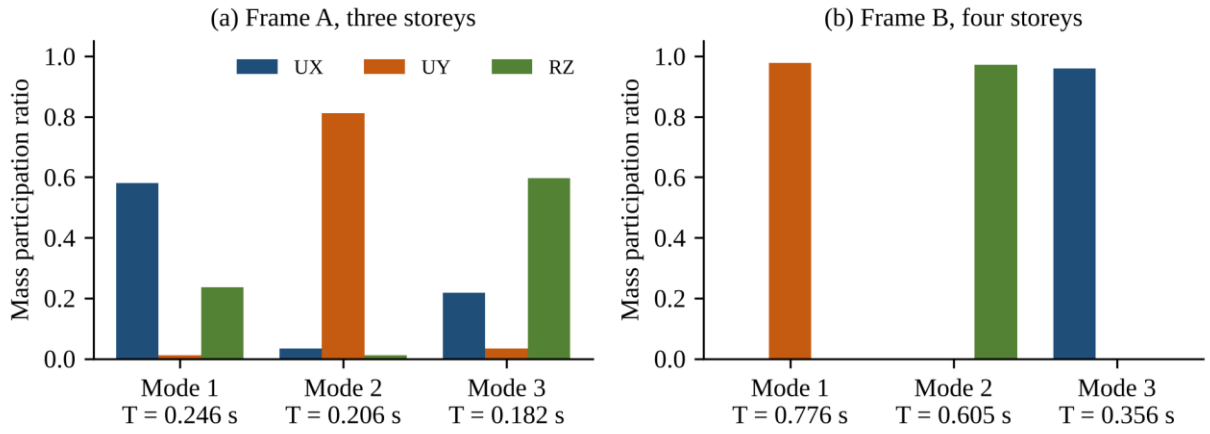


Fig. 5. Modal mass participation of the first three modes: (a) Frame A, (b) Frame B.

3.4 Storey stiffness of Frame B

The problem in Frame B is vertical. Fig. 6a shows that the ground storey retains only 47 percent of the Storey 2 lateral stiffness in X and 31 percent in Y. IS 1893 (Part 1):2016 defines a soft storey as one whose lateral stiffness is less than that of the storey above, and the Y-direction value is well below the 60 percent threshold that the earlier edition of the code used to mark an extreme soft storey. The drift profile follows directly (Fig. 6b). Under EQ Y the Storey 1 drift ratio reaches 8.88×10^{-3}, more than twice the code limit, whereas the storeys above stay between 1.1 and 2.2×10^{-3}. For Frame B, jacketing all ground-storey columns or adding stiffening elements in the Y direction is a global requirement and not only a durability repair, which agrees with comparative retrofit studies on soft-storey frames in India [21].

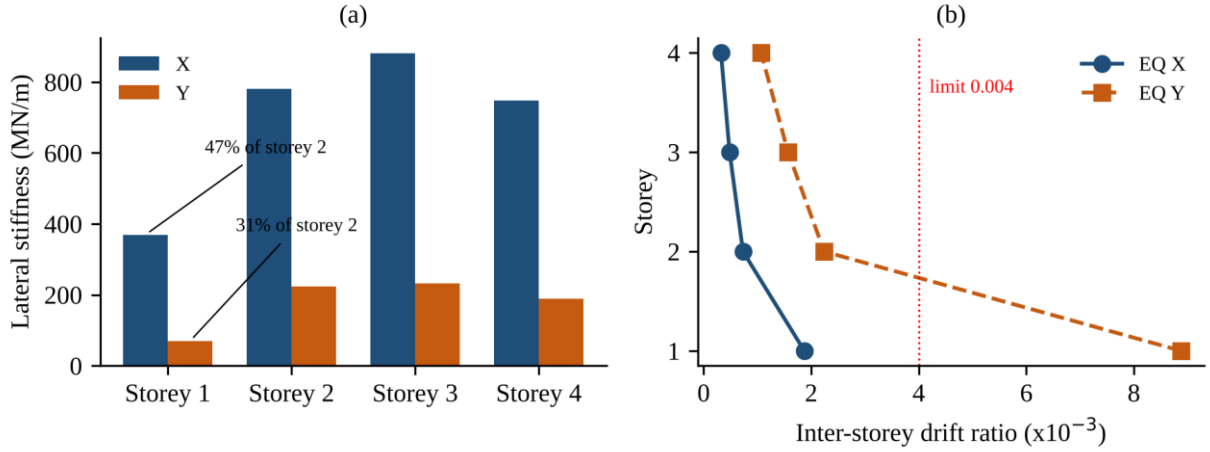


Fig. 6. Frame B: (a) lateral storey stiffness under EQ X and EQ Y, (b) inter-storey drift ratios.

IV. Capacity of the Critical Column under Corrosion

4.1 Method

The critical interior column of Frame A carries Pu = 1037 kN with a major-axis moment of 25 kN m. Its gross section is 225 mm × 525 mm with eight 16 mm bars (Asc = 1608 mm², 1.36 percent). Axial capacity was first checked with the short-column expression of IS 456:2000 [25]:

$$P_u = 0.4\, f_{ck}\, A_c + 0.67\, f_y\, A_{sc} \tag{1}$$

where Ac is the net concrete area. The minimum eccentricity, emin = l/500 + D/30, is 23.5 mm about the major axis and 13.5 mm about the minor axis. The second value exceeds 0.05D, so Eq. (1) alone is not sufficient and a biaxial check was carried out with a minor-axis moment of Pu × emin = 14.0 kN m, where αn is taken from Puz:

$$(M_{ux}/M_{ux1})^{\alpha n} + (M_{uy}/M_{uy1})^{\alpha n} \le 1.0 \tag{2}$$

$$P_{uz} = 0.45\, f_{ck}\, A_c + 0.75\, f_y\, A_{sc} \tag{3}$$

Uniaxial capacities Mux1 and Muy1 at the design axial load were read from interaction curves built by a fibre-based strain-compatibility routine using the IS 456 parabolic-rectangular stress block and an elastic-perfectly

plastic steel law with fyd = 0.87fy. Four states were considered. S0 is the intact section. S1 represents early corrosion with 10 percent bar section loss and sound cover. S2 represents the condition observed in Fig. 3, with 25 percent bar loss and 40 mm of cover lost on both long faces. S3 is a bounding case in which steel is ignored entirely. Corroded bars were assumed to keep their yield stress, a simplification that tends to overestimate capacity once pitting becomes severe [4], [5].

4.2 Results

Results are listed in Table 1 and plotted in Figs. 7 and 8. The intact column is adequate, with an axial DCR of 0.90 and a biaxial interaction ratio of 0.58. The margin is thin, though. Fig. 8a shows that with sound cover the column crosses the demand line at about 25 percent bar loss. Once 40 mm of cover is lost on two faces, even slight corrosion pushes the column below the demand. State S2 gives an axial DCR of 1.12, and because the demand point now lies beyond the major-axis interaction curve at that load (Fig. 7b), the biaxial ratio rises to 5.55. Ignoring steel altogether (S3) gives a DCR of 1.46. That bound is useful as a sanity check but is too pessimistic to serve as a design basis.

Table 1. Capacity of the critical column for the corrosion states and jacket options (Pu = 1037 kN).

Case	Description	Asc (mm²)	Pu (kN)	Puz (kN)	Mux1 (kN m)	Muy1 (kN m)	Biaxial ratio	Axial DCR
S0	Intact section	1,608	1146	1287	63.0	21.6	0.58	0.90
S1	10% bar loss, cover sound	1,448	1103	1238	52.1	18.5	0.81	0.94
S2	25% bar loss, 40 mm cover lost	1,206	929	1043	12.0	12.8	5.55	1.12
S3	Steel ignored (bound)	0	709	797	0.1	0.0	n.a. (P > Puz)	1.46
J75	75 mm M35 jacket on S2 core	2,564	3086	3469	379.8	190.4	0.12	0.34
J100	100 mm M35 jacket on S2 core	2,564	3779	4248	453.4	251.1	0.13	0.27

Note: Jacket values include the monolithic factor kM = 0.9. Moments at Pu = 1037 kN; jacket cases checked with minimum-eccentricity moments of the enlarged section (Mux = 29.6 kN m, Muy = 19.2 kN m for J75).

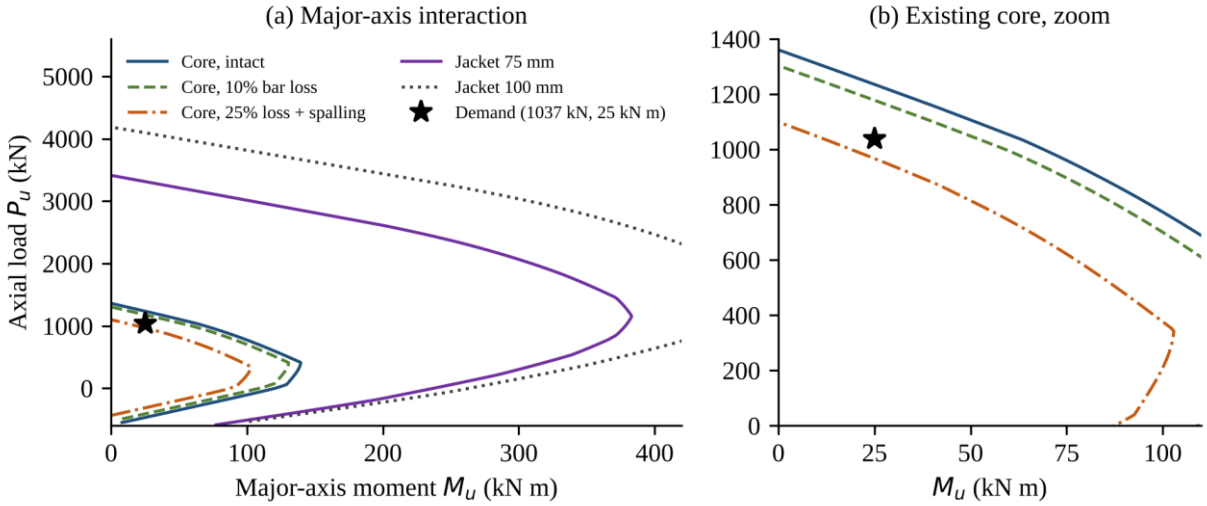


Fig. 7. Major-axis P-M interaction for the existing column at three corrosion states and for the jacketed sections: (a) full range, (b) close-up near the demand point.

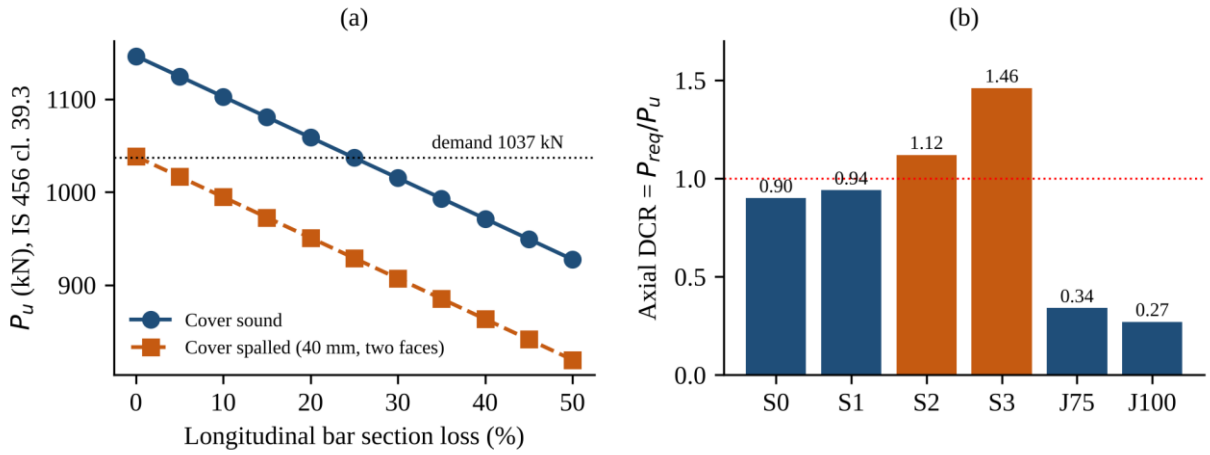


Fig. 8. (a) Axial capacity of the existing column against bar section loss, with and without cover spalling, (b) axial DCR for all cases in Table 1.

Two practical messages follow. First, the original design was not deficient. The column fails only because of deterioration, so the repair must at minimum restore the lost cover and steel. Second, a cover-only repair with polymer mortar would bring S2 back towards S1 but would leave a DCR of about 0.94 with no allowance for further section loss or for the imposed load that is missing from the archived model (Section 6). A jacket that adds capacity was judged the more defensible choice.

V. Micro-Concrete Jacket Design

5.1 Material selection

Pre-bagged micro-concretes differ widely in early shrinkage. Fig. 9 reproduces the data of Nayak et al. [16] for six commercial products. Mix F shows the largest 28-day free shrinkage (0.142 percent) and Mix D the largest 28-day differential shrinkage relative to the substrate (0.106 percent), while Mixes A and B show only 0.004 percent differential shrinkage at 3 days. Because interface cracking in [16] tracked the combination of relative shrinkage and bond strength rather than free shrinkage alone, the jacket specification called for a 3-day differential shrinkage below 0.01 percent, a minimum 28-day compressive strength of 35 MPa and a pull-off bond test on a site trial panel. The aggregate top size was limited to 10 mm so that the material could pass between the jacket bars and the old face.

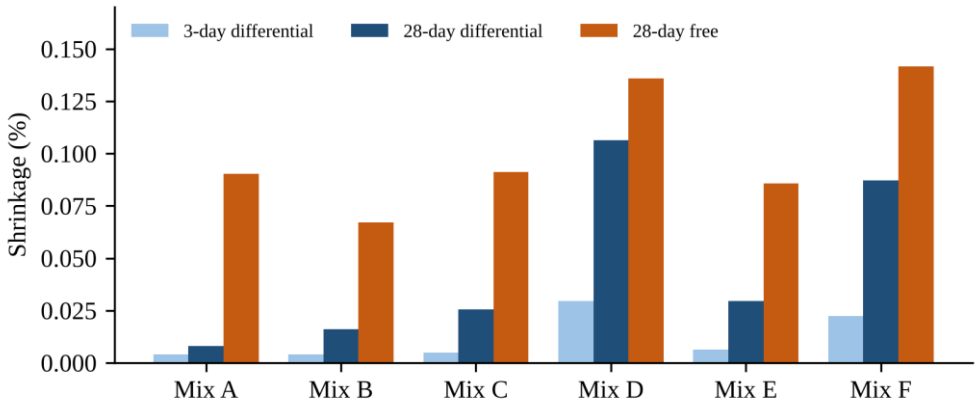


Fig. 9. Differential and free shrinkage of six cement-based micro-concretes (data from Nayak et al. [16]).

5.2 Jacket section and capacity

The jacket is 75 mm thick on all four faces, giving a 375 mm × 675 mm section (Fig. 10). It carries twelve 12 mm Fe415 bars and 8 mm closed ties at 100 mm centres, anchored into the slab and foundation by drilled and grouted dowels. IS 15988:2013 [28] recommends a minimum jacket thickness of 100 mm for conventional concrete. The 75 mm thickness was accepted on the basis of the flowable micro-concrete and the 10 mm aggregate size, and a 100 mm option was checked in parallel. Composite capacity was calculated with the core and jacket concretes assigned their own strengths and reduced by a monolithic factor kM = 0.9, in line with EN 1998-3 [30] and the approach of [23], [24]:

$$P_{u,j} = k_M\,[0.4\,f_{ck,c}\,A_{c,c} + 0.4\,f_{ck,j}\,A_{c,j} + 0.67\,f_y\,(A_{sc,c} + A_{sc,j})] \quad (4)$$

where subscripts c and j refer to the core and jacket. The corroded core of state S2 was retained in the calculation, and the cover concrete removed during break-out was counted as jacket concrete. The 75 mm jacket gives Pu,j = 3086 kN and an axial DCR of 0.34. The biaxial ratio falls to 0.12 even after the minimum-eccentricity moments are recalculated for the larger section. The 100 mm option gives 3779 kN. Either section is adequate. A straightforward calculation that assigns M35 to the whole 375 mm × 675 mm area, which is sometimes seen in practice, would give about 3540 kN for this section and overstate the capacity by roughly 15 percent, because the 225 mm × 525 mm core is still M15.

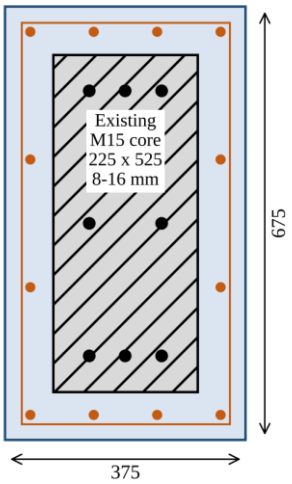


Fig. 10. Jacketed column section: existing M15 core with eight 16 mm bars and 75 mm M35 micro-concrete jacket with twelve 12 mm bars and 8 mm ties at 100 mm.

The jacket also changes the global behaviour. The column section stiffness increases by a factor of about 3.5 about the major axis. Because the jackets add stiffness where they are placed, the order and extent of jacketing can be arranged to pull the centre of rigidity toward the centre of mass and reduce the torsional ratio. The added dead weight of about 3.4 kN per metre of column height is small compared with the existing column loads. Jacketing columns selectively to correct torsional irregularity has been examined experimentally for hybrid jackets [22], and its effect on Frame A should be confirmed by response spectrum analysis, as IS 1893 requires for torsionally irregular buildings.

5.3 Execution and quality control

The repair sequence was as follows. The building was propped. Distressed concrete was broken out to at least 20 mm behind the bars, the bars were wire-brushed to a bright finish and coated with a zinc-rich primer, and any bar with more than about 25 percent section loss was supplemented with a lapped bar. The substrate was roughened and kept saturated surface-dry before a bonding agent was applied. The micro-concrete was then poured from one side of a sealed formwork until it emerged on the opposite face, which removes trapped air without vibration. Curing continued for at least seven days. Post-repair UPV readings reported by the site team exceeded 4.0 km/s, which falls in the "good" band of IS 516 (Part 5/Sec 1):2018. Table 2 compares the selected option with the main alternatives for this building.

Table 2. Qualitative comparison of column repair options for Frame A, based on [1]-[3], [8]-[14].

Option	Capacity gain	Section growth	Steel protection	Site skill / time	Relative cost	Fit for Frame A
Polymer-modified mortar patch	None	None	Moderate	Low / short	Low	Cover only; DCR stays near 1
Micro-concrete RC jacket	High	75 to 100 mm per face	High (alkaline cover)	Moderate / moderate	Moderate	Selected
Steel jacket (angles and battens)	Moderate	Small	Needs painting	Moderate / short	Moderate	Corrosion-prone in humid use
CFRP wrap	Low to moderate (axial)	Negligible	Seals surface only	High / short	High	Limited gain on 2.3:1 section
UHPFRC thin jacket	High	20 to 40 mm	Very high	High / moderate	High	Material not locally routine

VI. Discussion and Limitations

The two frames show why a building-level audit should come before member repair. In Frame A the global stiffness is ample and the deficiency is local, caused by corrosion of individual columns, together with a torsional irregularity that the repair can be arranged to reduce. In Frame B the ground storey is the weak link regardless of corrosion, so a member-by-member repair would leave the main risk untouched.

Several limitations apply. The archived ETABS models carry no imposed load, so the column demand reflects dead load and lateral actions only. Including live load to IS 875 (Part 2) would raise the axial demand and strengthen the case for jacketing. Equivalent static analysis was used even though IS 1893 calls for dynamic analysis in torsionally irregular buildings. The corrosion states are idealised. Pitting, loss of tie confinement and bar buckling, which governed capacity in recent tests on low-strength columns [4], [5], were not modelled. Finally, the shrinkage data in Fig. 9 come from the literature and not from the products used on site, so trial-panel testing is still needed.

VII. Conclusions

A staged audit and jacket design was applied to a corrosion-damaged three-storey M15 building in Mumbai, with a second four-storey frame used for comparison. The main conclusions are as follows.

(1) Frame A satisfies the IS 1893 drift limit by a factor of about six, but it is torsionally irregular in X, with $\Delta max/\Delta avg$ up to 1.33 and 24 percent rotational mass in the first mode.

(2) Frame B has a soft ground storey retaining 31 percent of the upper-storey stiffness in Y, and its Storey 1 drift ratio of 0.0089 exceeds the code limit by more than a factor of two. Its retrofit is a global problem.

(3) The intact critical column of Frame A is adequate (DCR 0.90). It becomes inadequate at about 25 percent bar section loss with sound cover, or at almost any corrosion level once cover spalls. With 25 percent loss and spalling the DCR is 1.12 and the biaxial check fails.

(4) A 75 mm M35 micro-concrete jacket with twelve 12 mm bars restores the column to an axial DCR of 0.34 and a biaxial ratio of 0.12. Treating the full jacketed section as M35 would overestimate axial capacity by about 15 percent, so the core and jacket concretes should be handled separately.

(5) Micro-concrete should be selected on early differential shrinkage and site bond tests, not on compressive strength alone.

Future work will extend the audit to response spectrum and pushover analysis of the jacketed frame, include imposed loads, and calibrate the corrosion scenarios against half-cell potential and cover-meter data collected on site.

Acknowledgement

The authors thank the building owner and the site repair team for access to the structure and for sharing the post-repair inspection records.

References

[1] M. Alghannam, M. Abdulqader, and A. Al-Fakih, "Jacketing techniques for repair and rehabilitation of RC column structures: A review," Struct. Durab. Health Monit., vol. 20, no. 5, 2026, doi: 10.32604/sdhm.2026.079454.

[2] S. Raza, M. K. I. Khan, S. J. Menegon, H. H. Tsang, and J. L. Wilson, "Strengthening and repair of reinforced concrete columns by jacketing: State-of-the-art review," Sustainability, vol. 11, no. 11, Art. 3208, 2019, doi: 10.3390/su11113208.

[3] A. Habib, U. Yildirim, and O. Eren, "Column repair and strengthening using RC jacketing: A brief state-of-the-art review," Innov. Infrastruct. Solut., vol. 5, no. 3, Art. 75, 2020, doi: 10.1007/s41062-020-00329-4.

[4] H. O. Aminulai, A. F. Robinson, N. Ferguson, and M. M. Kashani, "Impact of corrosion on axial load capacity of ageing low-strength reinforced concrete columns with different confinement ratios," Constr. Build. Mater., vol. 384, Art. 131355, 2023, doi: 10.1016/j.conbuildmat.2023.131355.

[5] H. O. Aminulai, A. Robinson, N. Ferguson, and M. M. Kashani, "Nonlinear behaviour of corrosion damaged low-strength short reinforced concrete columns under compressive axial cyclic loading," Eng. Struct., vol. 289, Art. 116245, 2023, doi: 10.1016/j.engstruct.2023.116245.

[6] H.-P. Chen, Y. Jiang, L. Xiao, and J. Liu, "Lifetime reliability analysis of concrete columns damaged by reinforcement corrosion," Front. Mater., vol. 9, Art. 926259, 2022, doi: 10.3389/fmats.2022.926259.

[7] K.-Y. Dai, X.-H. Yu, K. Qian, and D.-Y. Wang, "Deformation capacity of FRP retrofitted reinforced concrete columns with corroded reinforcing bars," Eng. Struct., vol. 254, Art. 113834, 2022, doi: 10.1016/j.engstruct.2021.113834.

[8] J. Chen, Z. Wang, A. Xu, and J. Zhou, "Compressive behavior of corroded RC columns strengthened with ultra-high performance jacket," Front. Mater., vol. 9, Art. 859620, 2022, doi: 10.3389/fmats.2022.859620.

[9] J. P. Tang, R. Feng, W. M. Quach, and J. J. Zeng, "Axial compressive behaviour of simulated corrosion-damaged RC columns retrofitted with UHPFRC jackets subjected to dry-wet cycling condition," Constr. Build. Mater., vol. 424, Art. 135956, 2024.

[10] M. A. Al-amoodi, M. Z. A. M. Zahid, B. A. Bakar, and A. M. Zeyad, "Behavior of damaged reinforced concrete columns retrofitted with ultra-high performance fiber reinforced concrete jackets under uniaxial loading," J. Build. Eng., Art. 112837, 2025.

[11] H. Shehab, A. Eisa, A. M. Wahba, P. Sabol, and D. Katunský, "Strengthening of reinforced concrete columns using ultra-high performance fiber-reinforced concrete jacket," Buildings, vol. 13, no. 8, Art. 2036, 2023, doi: 10.3390/buildings13082036.

[12] M. D. Criado Fernández, S. Martínez De Mingo, and A. Almerich-Chulia, "Thin HPFRC jackets for axially loaded RC columns: Mechanical behavior and efficacy of strengthening," Materials, vol. 19, no. 2, Art. 220, 2026, doi: 10.3390/ma19020220.

[13] R. Labdaoui, A. Toukal, and M. Kadri, "Effect of thin fiber-concrete jacketing on the resilience of damaged RC columns," Rev. Constr., vol. 24, no. 3, pp. 706-719, 2025, doi: 10.7764/RDLC.24.3.706.

[14] F. Narlitepe, N. Kian, U. Demir, C. Demir, and A. Ilki, "A novel hybrid thin jacketing method for seismic retrofitting of substandard reinforced concrete columns," Eng. Struct., vol. 342, Art. 120879, 2025, doi: 10.1016/j.engstruct.2025.120879.
[15] S.-G. Hong, J.-H. Lee, Y. Choi, and I.-Y. Gu, "Seismic strengthening of concrete columns by ultrahigh-performance fiber-reinforced concrete jacketing," J. Struct. Eng., vol. 147, no. 10, Art. 04021157, 2021, doi: 10.1061/(ASCE)ST.1943-541X.0003111.
[16] D. R. Nayak, R. R. Pattnaik, and B. C. Panda, "Study on relative shrinkage of cement-based micro-concrete for durable concrete repair," Clean. Eng. Technol., vol. 8, Art. 100444, 2022, doi: 10.1016/j.clet.2022.100444.
[17] H. Baloch, S. Grünewald, and S. Matthys, "Assessment of shrinkage and bond behaviour of high performance cement-based composites as a repair mortar," Dev. Built Environ., vol. 15, Art. 100203, 2023, doi: 10.1016/j.dibe.2023.100203.
[18] H. Liu, H. Zou, J. Zhang, J. Zhang, Y. Tang, J. Zhang, Y. Guo, and J. Xiao, "Interface bonding properties of new and old concrete: A review," Front. Mater., vol. 11, Art. 1389785, 2024, doi: 10.3389/fmats.2024.1389785.
[19] S. Mokhtari and M. Hassan, "Performance of bond between old and new concrete layers: The effective factors, durability and measurement tests, a review," Infrastructures, vol. 9, no. 10, Art. 171, 2024, doi: 10.3390/infrastructures9100171.
[20] M. R. Shendkar, A. Tantri, and A. U. Rao, "Seismic evaluation and retrofit of reinforced concrete structures," J. Infrastruct. Preserv. Resil., 2025, doi: 10.1186/s43065-024-00114-y.
[21] R. S. Patel et al., "Seismic performance assessment of a soft-storey RC building retrofitted with steel bracing, RC jacketing, and RC shear wall," Eng. Technol. Appl. Sci. Res., 2025.
[22] K. M. Ro, M. S. Kim, and Y. H. Lee, "An experimental study on torsional behavior of reinforced concrete columns retrofitted with hybrid concrete jackets," Materials, vol. 16, no. 3, Art. 1256, 2023, doi: 10.3390/ma16031256.
[23] G. E. Thermou, S. J. Pantazopoulou, and A. S. Elnashai, "Flexural behavior of brittle RC members rehabilitated with concrete jacketing," J. Struct. Eng., vol. 133, no. 10, pp. 1373-1384, 2007.
[24] G. Minafò, "A practical approach for the strength evaluation of RC columns reinforced with RC jackets," Eng. Struct., vol. 85, pp. 162-169, 2015, doi: 10.1016/j.engstruct.2014.12.025.
[25] Plain and Reinforced Concrete: Code of Practice, IS 456:2000, Bureau of Indian Standards, New Delhi, India, 2000.
[26] Criteria for Earthquake Resistant Design of Structures, Part 1: General Provisions and Buildings, IS 1893 (Part 1):2016, Bureau of Indian Standards, New Delhi, India, 2016.
[27] Design Loads (Other than Earthquake) for Buildings and Structures, Part 3: Wind Loads, IS 875 (Part 3):2015, Bureau of Indian Standards, New Delhi, India, 2015.
[28] Seismic Evaluation and Strengthening of Existing Reinforced Concrete Buildings: Guidelines, IS 15988:2013, Bureau of Indian Standards, New Delhi, India, 2013.
[29] Hardened Concrete: Methods of Test, Part 5: Non-Destructive Testing of Concrete, Section 1: Ultrasonic Pulse Velocity Testing, IS 516 (Part 5/Sec 1):2018, Bureau of Indian Standards, New Delhi, India, 2018.
[30] Eurocode 8: Design of Structures for Earthquake Resistance, Part 3: Assessment and Retrofitting of Buildings, EN 1998-3:2005, CEN, Brussels, Belgium, 2005.